Using remote sensing to quantify fishing effort and predict shorebird conflicts in an intertidal fishery

Clarke, L. J.[1], Hill, R.A. [2], Ford, A. [2], Herbert, R. J. H. [2], Esteves, L. S.[2], Stillman, R. A. [2]

1. School of Ocean Sciences, Bangor University, Menai Bridge, LL59 5AB.
2. Department of Life and Environmental Sciences, Bournemouth University, Christchurch House, Talbot Campus, Poole, BH12 5BB.

Corresponding Author: Leo Clarke

Email: l.clarke@bangor.ac.uk

Tel: +447725890589

ORCID: 0000-0002-1600-6197

Figures requiring colour printing: Figure 1, Figure 2, Figure 3, Figure 4.

Competing interests: None.

Funding: This work was part of a PhD project conducted at Bournemouth University, funded by the Southern Inshore Fisheries and Conservation Authority and Natural England.

Abstract

Accurate estimates of fishing effort are necessary in order to assess interactions with the wider ecosystem and for defining and implementing appropriate management. In intertidal and inshore fisheries in which vessel monitoring systems (VMS) or logbook programmes may not be implemented, quantifying the distribution and intensity of fishing can be difficult. The most obvious effects of bottom-contact fishing are often physical changes to the habitat, such as scarring of the sediment following dredging or trawling. We explored the potential of applying remote sensing techniques to aerial imagery collected by an unmanned aerial vehicle, or drone, in an area of intertidal mud flat (0.52 km^2) in Poole Harbour, UK, where shellfish dredging is widely carried out and conflicts between commercial fishing interests and the conservation of internationally important shorebird populations are a concern. Image classification and image texture analysis were performed on imagery collected during the open dredge season in November 2015, in order to calculate measures of fishing intensity across three areas of the harbour subject to different management measures. We found a significant correlation between results of the image texture analysis and official sightings records collected during the dredging season, indicating that this method most accurately quantified dredging disturbance. The relationship between shorebird densities and food intake rates and the results of this analysis method were then investigated to assess the potential for using remotely sensed measures of fishing effort to assess responses of overwintering shorebird populations to intertidal shellfish dredging. Our work highlights the application of such methods, providing a low-cost tool for quantifying fishing effort and predicting wildlife conflicts.

Keywords: remote sensing; unmanned aerial vehicle; intertidal; dredging; shellfishing; shorebirds

1. Introduction

In an era of rapid biodiversity loss and anthropogenic change, remote sensing is increasingly used to aid environmental management and conservation by identifying links between remotely detectable environmental parameters and patterns of biodiversity and species abundance (Turner et al., 2003; Nagendra et al., 2013). Such approaches are most frequently applied in terrestrial environments to monitor ecological responses to changing patterns of land use and land cover (LULC). Yet work is increasingly exploring the potential application of remote sensing in coastal and marine systems where multiple human activities require careful management, particularly in protected areas (Nagendra et al., 2013).

In the marine environment, fishing represents one of the largest sources of disturbance and management must reconcile the impacts of commercial harvesting with the interests of conservation. Many inshore fisheries target benthic invertebrates such as shellfish and marine worms, which necessarily require the use of bottom-contact gears that can reduce the abundance and density of target and non-target species (Collie et al., 2000; Kaiser et al., 2006; Clarke et al., 2017) and elicit physical impacts to the environment (Martin et al., 2014). Inshore harvesting may therefore compete with highly protected shorebird populations for shellfish or worm prey (Goss-Custard et al., 2006; Bowgen et al., 2015), and there have been well-documented conflicts between such inshore fisheries and the interests of shorebird conservation (Atkinson et al., 2003; Verhulst et al., 2004; Ens, 2006).

Accurate estimates of the distribution and intensity of fishing are highly valuable when assessing fishing interactions with the wider ecosystem and defining and enforcing protected areas. Various data types to describe fishing effort may be collected, such as interviews with fishermen, market data, official catch statistics, surveys, sightings records and logbook data (McCluskey and Lewison, 2008). Obtaining such data in small-scale, artisanal and inshore fisheries, however, is often difficult. In offshore and larger fisheries detailed data on vessel movements is obtained from vessel monitoring systems (VMS) that can be used to produce detailed maps of fishing activity and effort. Techniques such as side-scan sonar, bathymetric light detection and ranging (LiDAR) and multi-beam echo sounders (MBES) (Kenny, 2003) can detect trawl marks or dredge scars on the seabed. Inshore and intertidal fisheries, however, are often exploited by smaller vessels in small-scale local fisheries for which VMS or logbook data are not compulsory (e.g. Clarke et al., 2018), and accurate estimates of effort and distribution prove difficult to obtain.

In intertidal fisheries the gears utilised often leave significant scarring of the sediment when exposed at low tide (Clarke et al. 2018), areas which may be easily accessed and photographed using unmanned aerial systems (UAS) (also known as drones, unmanned aerial vehicles (UAVs) and remotely piloted aircraft (RPA)). This imagery represents valuable data to which remote sensing techniques are often applied. The conspicuousness of this scarring coupled with the increased availability and affordability of UAS technology may therefore provide a potentially accessible and low-cost approach for obtaining data on the extent and intensity of bottom-fishing disturbance in intertidal habitats. Past studies have utilised aerial imagery and remote sensing techniques to map intertidal habitat extents (Thomson et al., 2003), to monitor intertidal morphological changes (Mason et al., 2010) and to quantify propeller scarring in shallow subtidal seagrass beds (Robbins, 1997; Dunton and Schonberg, 2002; Phinn et al., 2008), although their use in assessing impacts of bottom-contact fishing remains largely untapped.

Two commonly applied methods in ecological studies are image classification and image texture analysis. Image classification of raster data is an often-used remote sensing technique for characterising LULC and habitat mapping. Image classification can be broadly grouped into two methods: unsupervised classification, whereby the classification aims to group together data from a multiband raster according to their relative spectral qualities with no user intervention, or supervised classification, in which data are allocated according to their similarity to pre-defined, user characterised classes (Foody, 2002). Image texture has previously been used in terrestrial ecological studies as a proxy for vegetation structure and habitat complexity (Wood et al., 2012). Wood et al. (2013) built on this application of texture analysis, exploring the efficacy of image texture derived from Landsat TM satellite imagery and infrared aerial photography as a predictor of habitat quality and associated avian species richness.

The present study assessed the efficacy of the two approaches of image analysis - image classification and image texture - in accurately quantifying the spatial extent and intensity of shellfish dredging in intertidal mudflats based on the presence of dredge scarring in aerial imagery collected from a designated protected area. Following validation of each measure using routinely collected fishing sightings, the relationship between the most accurate measure and the distribution and feeding behaviour of key shorebird populations was investigated. Such methods may represent valuable tools for fisheries managers in accurately and effectively assessing fishing disturbance, with potential implications for management.

2. Methods

2.1 Study Area and Fishery

The study was carried out in Poole Harbour (Lat/Long: 50.6796, -2.0238), on the south coast of the UK in north-west Europe. Poole Harbour is a micro-tidal estuary with large extents of intertidal mudflats, sandflats and saltmarsh. The estuary is a designated Special Protection Area (SPA) under the European Birds Directive (2009/147/EC) due to its important breeding and non-breeding bird assemblages.

Poole Harbour supports a fishery of local economic importance for the non-native Manila clam *Ruditapes philippinarum* and the common cockle *Cerastoderma edule*, which are harvested using a unique 'pump-scoop' dredge. This was developed by local fishermen for use in intertidal and shallow subtidal areas and its defining characteristic is a pump powered by the engine of the vessel that pumps seawater through the back of the dredge, rinsing sediment from the dredge whilst in use (Jensen et al., 2004; Clarke et al. 2018). At low water, spiral scarring typical of such shellfishing gears can be seen clearly in intertidal mudflats, ranging from around 5 to 12 metres in diameter (Figure 1). A previous study identified a reduction in fine sediment content in areas following heavy dredging (Clarke et al., 2018). In 2015, a byelaw was introduced to regulate dredging within the harbour, with a zonation of permitted dredging intensity (Table 1). In addition to supporting this significant commercial fishery, the introduced Manila clam also supports overwinter survival of molluscivorous bird predators within the harbour, such as Eurasian oystercatcher *Haematopus ostralegus* and Eurasian curlew *Numenius arquata* (Caldow et al., 2007), and there is therefore concern regarding impacts of the fishery on overwintering bird populations.

The study was carried out in Wytch Lake, an intertidal area of 0.52 km^2 within Poole Harbour that is subject to pump-scoop dredging and encompasses three areas subject to different management regimes. The intertidal habitats within the study area as classified according to Connor et al. (2004) largely comprise polychaete and bivalve dominated mid estuarine muds and *Hediste diversicolor* and *Macoma balthica* in littoral sandy mud (Herbert et al., 2010). The outer extent of Wytch Lake is open to dredging all season (May – December) and has historically been dredged intensively by fishermen (i.e. chronic dredging). The middle section of the site is open to short-term (i.e. acute) dredging from July to October, while all commercial dredging activity is prohibited in the southern part of the site in the upper reaches of Wytch Lake (i.e. control conditions). The study site and management areas are presented in Figure 2, with the levels of fishing pressure summarised in Table 1. Fishing intensity in each management area was derived from Southern Inshore Fisheries and Conservation Authority (SIFCA) sightings data and discussions with local fishermen.

2.2 Bird Surveys

To assess the distribution and density of shorebirds, bird observations were conducted between September 2015 and March 2016. The site was visited twice a month on a low spring tide, with the exception of October 2015 when only a single count was conducted. On each visit, counts of each species present were made, along with detailed individual observations of the most abundant species present throughout the study area. This was done across all management areas subject to different levels of dredging effort throughout the 2015/16 winter. In order to expedite counts, each management area was subdivided into smaller survey ‘sectors’, defined by local features such as saltmarsh or channel boundaries (Figure 2). These sectors were labelled according to their dredging intensity (CH: chronic, long-term dredging; AC: acute, short-term dredging; and CN: control conditions, no commercial dredging) and numbered (Figure 2).

Each survey was conducted on a low tide of 0.9m or lower and as close to the lowest spring tide as permitted by daylight hours. A Swarovski STS 80 HD spotting scope was used to record birds from distances of 50 – 500m (depending on the survey patch). Bird numbers in each survey patch were counted every half hour, starting from one hour prior to low tide to one hour after low tide. The species most consistently present during the study period and for which density data were subsequently analysed were oystercatcher *Haematopus ostralegus*, curlew *Numenius arquatus*, black-tailed godwit *Limosa limosa*, Common redshank *Tringa totanus* and Common shelduck *Tadorna tadorna*.

In the time between the half-hourly species counts, videos of individual birds were recorded using a Pentax K-30 D-SLR camera and a Swarovski Telephoto Lens System to fit the camera to the spotting scope. Each individual bird was recorded for a period of 90 seconds. Feeding rates (or prey capture rates) were calculated as the number of times a bird swallowed a prey item per 90 seconds. These feeding observations were carried out for oystercatcher *Haematopus ostralegus*, curlew *Numenius arquata* and black-tailed godwit *Limosa limosa islandica*, a species for which Poole Harbour receives SPA designation. These represent the larger and more abundant species present within the site that are easily recorded at distance. The capture of prey is easily identifiable for these species due to the characteristic head movement involved in swallowing.

2.3 Intake Rates

To estimate intake rates for the three bird species, invertebrate data collected in November 2015 from each management area as part of a separate study was used (Clarke et al., 2018). Intake rates were calculated as the recorded feeding rates for each species multiplied by a weighted average prey mass. This was based on the relative abundance of prey items from November 2015 within each prey size class in each species diet, as reported by Goss-Custard et al. (2006). This weighted average ash-free dry mass (AFDM) (M) in grams, across all prey size classes that could potentially be consumed by each bird species, was calculated by first using:

$$\mathrm{M} = \sum_{i=1}^{n} p_i m_i$$

Where n = number of size classes, p_i = proportion of size class i (i.e. numerical abundance of size classes divided by the total numerical abundance of all prey size classes that could potentially be consumed), and m_i = published ash-free dry mass value for size class i. This approach assumes that birds consumed prey size classes in proportion to their abundance. The AFDM values were published values that have been used in a number of previous modelling studies that have used individual-based models (IBMs) to predict the effects of environmental change on wading birds (Stillman et al., 2001; Durell et al., 2006; Bowgen et al., 2015). The weighted average was then used to estimate the intake rates of individuals from each species based on the feeding rate observed through video analysis (i.e. feeding rate multiplied by the weighted average intake). As core sampling of the invertebrate assemblage was conducted in a grid design and did not cover the whole of each management area, this weighted average was extrapolated across all survey sectors within each of the three dredge management areas. With the caveat that these provide only an estimate of intake rates that may vary between locations throughout the study area over time, intake rates were compared for each species across dredging intensities as an indication of dredging impacts on energetic intake.

2.4 Aerial Survey

Given the sub-division of each management area into survey sectors, it was considered preferable to quantify fishing effort for each survey sector to allow a more detailed assessment, rather than to broadly compare shorebird responses across management areas. Therefore, a drone survey was undertaken to obtain aerial imagery across the study site from which estimates of fishing intensity could be derived.

At low tide (spring tide, LW 13:25, Height 0.5m) on 23rd November 2015 a DJI Phantom 3 Pro quad-copter Unmanned Aerial System (UAS) was flown over the study site using the Drone Deploy application (Drone Deploy, 2018). This was flown in a conventional aerial survey pattern of parallel flight lines to acquire vertical stereo aerial photographs (VSAP). The orientation, length and spacing of this flight was designed to account for wind direction and strength (to minimise drift and crabbing and abrupt changes in altitude due to gusting of winds) and to ensure photo overlap of at least 70% along-track and 30% cross-track. All flights were undertaken with wind speeds less than 15 mph and at the maximum permissible altitude of 400ft (122m).

A total of 1,191 (12-megapixel) images were acquired in JPEG format and processed using structure from motion and multi-view stereo photogrammetry (SfM-MVS) in Agisoft Photoscan Professional v1.4.2. Texture and pattern were abundant in photographs covering the shoreline but lacking in the majority of images which covered the intertidal mud flats.

Initial exterior orientation of individual photographs was estimated using six degrees-of-freedom (DoF) ephemeris data (i.e. eastings, northings, elevation, kappa, phi and omega). This was provided from the navigation-grade Global Navigation Satellite System (GNSS), digital compass and accelerometers onboard the Phantom 3 Pro and stored within the JPEG format imagery (in EXIF format). The relative exterior orientation was also initiated in the same way using SfM and refined using sparse cross-correlation image-matching based on all six DoF. Un-matched photographs from this process were rejected, with 1,049 remaining. The resulting sparse point cloud of tie points identified across multiple images was culled based on numbers of cross-correlated photographs, reprojection error, reprojection uncertainty and projection accuracy per point. Camera calibration, location and orientation were then optimised based upon the remaining 145,496 tie points, using a bundle adjustment (i.e. minimising the errors between image locations of observed and predicted image points using non-linear least-squares analysis across all images in the “bundle”, as summarised by Triggs et al. (1999)).

Dense cross-correlated image-matching was then used to create a dense point cloud of 323,491,411 points, identified in multiple images from multiple view angles. From this method each point has an x, y and z coordinate, from which a triangular irregular network (TIN) mesh of 64,520,192 faces and a digital elevation model (DEM) of 6.5cm ground sample distance (GSD, or cell size) was produced. This was used to ortho-rectify each image. The resulting orthophotographs were mosaicked and reprojected to Ordnance Survey British National Grid (OS BNG) projection, using Airy Spheroid (1936).

The resulting 24-bit red, green and blue (RGB) orthophotograph mosaic had a GSD of 3.05cm. Due to mud flats dominating the imagery, with associated safety concerns and limited tidal windows, it was not deemed feasible to collect ground control points (GCPs) which could be used either in the process of ortho-rectification or to validate the geometric accuracy of the derived output. Therefore, it was only possible to perform exterior orientation based on the aforementioned 6 DoF ephemeris. For this reason, the theoretical absolute locational uncertainty of each pixel is +/- 3m, although in reality the bundle adjustment is likely to have improved this considerably (but by an unquantifiable level). The relative locational uncertainty is likely to be considerably better and of the order of a few pixels (i.e. approximately 12cm).

The mosaicked images were loaded into a Geographical Information System (GIS) (ArcMap v10.1) for analysis. The image was then clipped to the extent of the intertidal habitat within the study site and divided into nine separate survey polygons. These were sub-divisions of the study area in which monthly bird observations had been carried out during the winter of 2015/2016 (Figure 2).

2.5 Image Analysis

2.5.1 Image Classification

Areas of no data were removed prior to analyses being undertaken. First, an unsupervised classification was performed on the aerial imagery of the intertidal extent of the study area, clipped to each survey sector. The unsupervised classification process allocates image pixels into classes according to their individual spectral values. The user defines the maximum number of output classes into which pixels are allocated, which is often set at approximately 10 times the number of bands in the input raster (ESRI, 2018). A maximum of 30 output classes were therefore specified for the unsupervised classification process. In order to expedite the analysis process and overcome small-scale variation in reflectance across the mosaic this process was performed on aerial imagery clipped to each survey sector separately.

Next, for pixels representing exposed mudflats in the estuary, each of the output pixel classes was manually allocated into one of three groups: 1 – scarred sediment; 2 – a combination of scarred and naturally disturbed sediment; 3 – undisturbed sediment. This process was done iteratively using best judgement, by highlighting an individual output class from the image classification process and determining whether pixels within that class represented either: scarred sediment as a result of pump-scoop dredging (i.e. physically disturbed sediment through fishing effort); undisturbed sediment; or a combination of artificially (i.e. by dredging) and naturally (i.e. by seafloor geomorphological processes) disturbed sediment. It was decided during initial exploratory analysis that using three groups was the optimal approach; in some cases a single pixel class was mixed in its composition, representing spatially separated areas of both artificially and naturally disturbed sediment. Areas such as this were grouped separately within the middle group in order to account for this uncertainty and ensure a conservative approach. Such uncertainty may result from, for example, geomorphological processes along creeks and channels, natural hydrodynamic processes and gradients in sediment characteristics across shore heights, and partial physical recovery of older scars. These three groups and the criteria for their selection are summarised in Table 2.

Once pixel classes had been grouped together, the reclassify tool was used to create three new classes based on the new groups. For each of the survey sectors in which bird observations were carried out, the area of each of these new output classes was then calculated using the calculate geometry tool, to quantify the area of sediment affected by dredging activity. For these calculations a scale factor was assigned to each group based on the confidence in the classification in correctly characterising disturbed sediment due to dredging activity, and the absolute area of each class was then multiplied by the corresponding scale factor (Table 2). This accounted for the uncertainty in the second group, taking a conservative approach in applying a scale factor of 0.5 to this group.

2.5.2 Texture Analysis

Image texture analysis was also carried out on the aerial imagery using the focal statistics tool in ArcMap 10.1. Neighbourhood analysis was performed, whereby a value is calculated for each cell, or pixel, in the output raster as a function of the original pixel values within a specified ‘neighbourhood’ surrounding that pixel. In this case a measure of variety, or ‘pixel diversity’, was assigned to each image pixel. This was calculated as the number of unique pixel values in a surrounding grid of a specified size, thus providing a measure of image texture. This neighbourhood analysis used a moving window (kernel) of 200 x 200 pixels, or 7 x 7m, thereby covering an area of 49m^2. Given that the diameter of dredge scarring from the image was generally measured as between 5 and 12 metres, this covered sufficient area to capture any variation in sediment spectral characteristics due to dredging activity. Pixel values in the output raster therefore represent the diversity in the pixel values across the surrounding 49m^2 of mudflat. The *x* and *y* position of the processing pixel in the grid was determined by:

X = (width of neighbourhood +1) / 2

Y = (height of neighbourhood +1) / 2.

Pixel diversity values from the raster output from the neighbourhood analysis were then summarised for each of the survey sectors using the zonal statistics tool. These could then be used to compare relative texture across the study area as a surrogate for dredging effort; a higher mean pixel diversity value was taken as indicative of increased habitat heterogeneity and sediment disturbance.

2.6 Statistical Methods and Comparison and Validation of Methods

One-way ANOVA was performed on pixel diversity measures to compare values between survey sectors. In order to compare the two methods of image analysis a Spearman's rank correlation was carried out on the results for each of the nine survey sectors. The strength with which each method relates to the known distribution of dredging effort was then investigated by performing a Kendal's correlation of the number of SIFCA patrol sightings in each survey sector from 2011 to 2015 with the results from each of the methods. This method provides an estimate of Kendall's tau-b correlation coefficient, which is more effective when there are ties within the data. This was the case here as in four of the sectors no sightings were observed.

2.7 Relating Shorebird Responses to Dredging Intensity

Following validation, the most accurate measure was carried forward in order to investigate the relationship between fishing intensity and both bird species distribution and feeding/intake rates using a generalised linear model (GLM) framework. Species distribution patterns were investigated for Eurasian oystercatcher, Eurasian curlew, black-tailed godwit, redshank *Tringa totanus* and shelduck *Tadorna tadorna*; the species most abundant throughout the winter and for which sufficient count data was obtained. The appropriate error distribution for each species model was determined based on the over-dispersion parameter (theta) and the distribution of model residuals. The Akaike Information Criterion (AIC) value and diagnostic plots for each model were then taken as indicative of model quality. In this analysis each half-hourly count during each survey was treated as a replicate. The number of days through the winter (from the first survey on 02/09/2015) and/or the height of low water were also included as covariates to account for residual variation where AIC values indicated a better model fit when included.

2.8 Statistical Notes

Pseudoreplication is evident in the dataset as for each survey patch there is only one measure of fishing intensity and the same value re-occurs each time the patch is analysed, resulting in non-independence. Furthermore, long-lived shorebirds such as the species observed in this study display strong between-year and season-long site fidelity (Ens and Goss-Custard, 1986; Marks and Redmond, 1996; Finn et al., 2001). Therefore, the birds observed in each fortnightly count are to likely be the same individuals and hence also non-independent (Zharikov and Skilleter, 2004). However, introducing random-effects or repeated measures into the model to account for this would reduce the analysis down to impractical degrees of freedom. The GLM approach allows the appropriate error structure and link function to take into account the over-dispersion and the heterogeneity of variance in the data due to non-independence, and is considered the best option here. The models used in our analyses therefore represent the best fit models that deal with these issues while allowing for a biologically reasonable analysis to be undertaken, identifying the broad trends between species distributions, feeding rates and intake rates and fishing intensity.

3. Results

3.1 Image Classification

Outputs of the image classification show that dredging effort is mainly concentrated in the outer reaches of the study site (Figure 3). Inset on Figure 3 are magnified images of areas broadly characterised by each of the three output classes. Dredging effort in the area opened to dredging in 2015 appears to be at similar levels to the heavily dredged area subject to chronic dredging pressure (Figure 5; Table 3). The extent of scarring in the northern-most section of the heavily dredged site (CH1) appears relatively low however, comparable to levels of scarring observed in the control site (Figure 5). While no commercial fishing activity was observed by SIFCA in the control site during the study period, low levels of scarring are evident in the results.

3.2 Image Texture

Outputs of the image texture analysis (Figure 5) indicate that pixel diversity values, as a proxy for sediment disturbance, follow the same broad trend as those from the image classification methods (Table 4; Figure 6). Taken as estimates of image texture, higher values of pixel variety, or diversity, are attributed to the site subject to chronic fishing pressure and a decreasing trend occurs towards the control site at the upper reaches of the channel, where the lowest mean values are observed. This indicates that image texture is generally greater in those areas subject to more intense fishing, although some of the AC (short-term fishing) survey sectors appear to show areas of relatively low diversity values compared to the extent of scarring identified through the image classification technique. Standard deviations are presented (Figure 6) as standard errors of pixel values are too small to be visible when plotted (Table 4) due to the large sample size deriving from the number of pixels in the high resolution imagery. One-way ANOVA indicates high significance between pixel diversity values between survey sectors ($F (8, 430109098) = 12046456.95$, $p < 0.0001$).

The range of pixel diversity values is lowest in the control sectors and highest in sectors in the site dredged most intensely. The largest range is observed in sector CH3, consistent with the largest extent of scarring identified through the image classification process. Conversely however, sector CH1 shows the second highest range of pixel values, in contrast to the lowest extent of scarring identified through image classification of all sectors. This may be due to areas of high variance in pixel diversity and sediment characteristics (Figure 5) within this sector being grouped in the middle pixel class through image classification, potentially underestimating the extent of scarring.

3.3 Comparison and Validation of Methods

There is no correlation between the results of the two analyses (percentage of scarred sediment vs. mean pixel diversity) (Figure 7a) ($rs = 0.21$, $p = 0.58$). However, with CH1 removed from the analysis, the sector in which scarring was lowest and a clear outlier in the scatterplot, a significant correlation between the outputs of the two methods is evident ($rs = 0.74$, $p < 0.05$).

A significant positive relationship between the number of sightings of dredge activity in each survey sector and the mean pixel diversity is evident (Figure 7b) ($tau = 0.81$, $p < 0.001$), but there is no significant relationship with the percentage of scarred sediment (Figure 7c) ($tau = 0.09$, $p = 0.75$). This suggests that the image texture approach more accurately represents the known distribution of fishing effort. With the outlier of CH1 removed this relationship is unchanged (pixel diversity vs. sightings: $tau = 0.75$, $p < 0.05$; scarring extent vs. sightings: $tau = 0.43$, $p = 0.15$). Pixel diversity values were therefore considered to best represent known fishing distribution from SIFCA official sightings data and were carried forward into the analysis of species densities and feeding/intake rates.

3.4 Species Distribution in Relation to Dredging Intensity

Numbers of all species were variable over the course of the winter and across the management areas.

The best-fitting models for each species are presented (Table 5). Oystercatcher, curlew, and shelduck all occur in higher densities in areas of higher dredging intensity, as represented by increased values of image texture, whereas densities of redshank and black-tailed godwit show no relationship with dredging intensity (Figure 8). A significant effect of the number of days through winter is evident on oystercatcher and redshank densities, with a decrease and increase in densities of each species respectively over time. The height of low water shows a significant effect on oystercatcher and curlew densities, which demonstrate an increase on higher tides (Table 5).

3.5 Feeding and Intake Rates

A total of 355 videos were recorded of oystercatcher ($n = 150$), black-tailed godwit ($n = 73$) and curlew ($n = 132$) throughout the study site. Species feeding rates across all survey patches were variable throughout the winter of 2015/16, although no difference between months is apparent for any of the species for which this data was collected (oystercatcher ($F(6,143) = 0.97$, $p = 0.45$); black-tailed godwit ($F(5,67) = 1.01$, $p = 0.42$); curlew ($F(6,125) = 0.86$, $p = 0.52$)). Data across all months were therefore pooled before further analyses were undertaken.

There is no significant effect of pixel diversity on oystercatcher feeding rates, although results show a significant positive effect on intake rates (Table 6), indicating that oystercatchers obtain more energy in areas of higher fishing disturbance across the study site during winter 2015/16. Feeding rates of black-tailed godwit however appear significantly lower in areas of higher sediment disturbance/pixel diversity (Table 6). The same trend is not evident in intake rates however; although the data shows a negative trend there is no significant effect on mean AFDM intake evident throughout the study area. Feeding and intake rates of curlew show a similar trend to black-tailed godwit, with significantly lower feeding rates observed in areas of higher sediment disturbance/pixel diversity, although again, however, this lower rate of feeding does not result in a reduction in AFDM intake (Table 6).

4. Discussion

Our results suggest that the methods used to analyse remotely obtained aerial imagery may provide accurate estimates of the extent and intensity of intertidal dredging, and demonstrates their application for conservation and management. Image classification methods may quantify the spatial extent of affected habitat, whilst image texture can provide a measure of sediment disturbance against which shorebird responses can be assessed. Whilst other techniques, such as geographic object-based image analysis (GEOBIA), combine the advantages of the two methods used here, such methods are suitable for discrete objects within the image (Blaschke et al., 2014). Due to the nature of the dredging, the scarring in the imagery overlaps significantly, through both the initial dredging process itself and repeated fishing over time. Given the complexity of the dredge scars (Figure 3), portioning the image according to the geometry, shape and texture of scarring is therefore considered unlikely to yield effective results.

With the outlier of sector CH1 excluded, for which results of the classification did not correspond to the image texture results, both methods appear equivalent, although when compared to official sightings data results suggest that pixel spectral diversity, and hence habitat heterogeneity/sediment disturbance, may be a more accurate measure of dredging disturbance than image classification results. Uncertainty in the classification method is accounted for by introducing a third class in which pixels represent scarred sediment in one place and naturally disturbed sediment in another. These inconsistencies likely arise due to the relative homogeneity of the habitat. Remote sensing techniques are generally applied at a much broader scale than that used in this study (Hall et al., 1991; Quattrochi and Goodchild, 1997) to identify LULC patterns or habitat extents over many hectares. Soft sediment intertidal mudflats and sandflats are comparably uniform habitats however, potentially affecting the accuracy with which the classification process can identify spectral differences.

Results from the classification process may be confounded by other sources of disturbance causing similar spectral values to those disturbed by pump-scoop dredging, such as natural hydrodynamic processes. Other confounding factors include the gradient in sediment characteristics at different shore levels and the pooling of water within scars, resulting in similar spectral values to natural channels and small creeks. The method used accounts for such inconsistencies, although the lack of a significant relationship between the extent of scarring calculated through this method and the fisheries sightings data demonstrates the potential inaccuracies. Low levels of sediment disturbance in the control site may indicate sediment disturbance from the processes described above, particularly as this area is close to a main channel, or perhaps more likely as a result of scarring from a SIFCA shellfish stock assessment in May 2015 and historic illegal fishing activity that has shown partial recovery. Whilst the analysis was performed separately for each survey sector, it is noteworthy that the only area in which some disparity across sector borders appears in Figure 3 is between sectors AC4 and CN2. This disparity appears to be largely accounted for in the higher areas of uncertainty in sector CN2 that may be driven by changes in sediment characteristics in the upper reaches of the study site (Clarke et al., 2018) and partial recovery of some scarring following the 2015 stock assessment. Results of the unsupervised classification appear consistent across all other sector borders however.

The notable discrepancy between the results of the two analysis methods in one of the historically dredged survey sectors (CH1) is likely due to areas of high variance in sediment characteristics (and therefore pixel diversity) (Figure 4) being grouped into the middle class during the image classification process, and therefore likely to be under-represented in the estimates of scarring extent. This survey sector does indeed have large areas of habitat categorised as Class 2 (Figure 3), which may explain the observed disparity, and with this removed from the correlation analysis a significant relationship between scarring and pixel diversity is observed. It is worth noting that fisheries patrols are not carried out at the same frequency at which fishing occurs. Patrols are carried out irregularly, although approximately weekly, and sightings data are likely to vastly underestimate fishing activity. If scarring extent was correlated with true fishing values in each sector a stronger relationship may be observed. However while VMS data is lacking these sightings are the best available data and pixel diversity most strongly correlates with this distribution of effort. The lower pixel diversity values in some of the AC sectors (subject to short-term dredging) derived from the image texture analysis appear contrary to the magnitude of dredge scarring quantified through the image classification methods. However, these areas of low pixel diversity may be those subject to heavy dredging, resulting in consistently disturbed sediments, and consequently similar pixel values across such areas.

The approach taken in this study required *a priori* information on the nature of the disturbance (i.e. the size of the spiral scarring) to decide on an appropriate scale at which to run the image classification analysis, and it is acknowledged that replication in this study is relatively low due to the number of survey sectors used. The site may have been divided into more sectors, perhaps using a gridded design. We propose that an investigation into the effect of scale over different grid sizes, particularly in image texture, would be worthwhile, as scale is an important consideration in remote sensing (Woodcock and

Strahler, 1987). However, the survey sectors were defined according to the design of the bird observations, with the aerial survey undertaken subsequently to provide an accurate estimate of scarring in each sector.

Our results demonstrate the potential for these methods to be integrated into an assessment of species abundance, distribution and functional responses to this kind of environmental disturbance. Previous work on the impacts of pump-scoop dredging on benthic communities in Poole Harbour (Clarke et al., 2018) showed a decline in bivalve molluscs and an increase in polychaetes and other opportunistic worms in areas of the study area due to dredging. It would therefore be reasonable to assume that those bird species for which bivalve molluscs comprise a key dietary component (e.g. oystercatcher, curlew (Goss-Custard et al., 2006)) would be more susceptible to the impacts of this kind of dredging. However results suggest that there is currently no effect of dredging pressure in determining species distribution patterns throughout the site. In fact, for the two species for which molluscs represent a significant prey item, oystercatcher and curlew, there appears a positive trend between dredging intensity and species densities. This preference for areas more disturbed by dredging potentially highlights that these birds depend on the same areas targeted by clam fishermen throughout the winter, in which case both may be competing for the same resource of bivalve prey. Given that in excess of 100% of a population’s winter food requirements needs to be maintained for population survival, due to the effects of competition and interference (Goss-Custard et al., 2004; Stillman and Wood, 2013), this spatial overlap of impact and conservation interests could be of concern should insufficient prey remain after the closure of the fishery in December, in particular the target species of the fishery (clams and cockles) for molluscivorous oystercatcher and curlew. Clearly there remains spatial and temporal overlap with the overwintering period for shorebird populations under the new management measures, and managers should remain vigilant that effort is controlled through the permit system to allow sufficient food to remain.

The height of low water on each survey, when included in the GLMs, had a positive effect on some species densities. Higher tides likely forces birds to feed higher up the shore and in a relatively smaller area, increasing bird densities. Black-tailed godwit however, a designated SPA species, appear to occur at lower densities on higher tides, potentially indicating that they leave the study area at these times. It may be that at higher tides when more of the study area is inundated, this species needs to leave the site to feed elsewhere to fulfil its daily energy requirements, which cannot be met in the upper reaches of the study area.

Despite lower feeding rates in heavily dredged areas for curlew and black-tailed godwit, this reduction does not translate to a significant reduction of AFDM intake; suggesting that prey in these areas is more profitable than in areas of lower dredging pressure where feeding rates are higher. Size of prey is a key determinant in the availability and profitability to bird predators, as birds cannot consume individuals above certain sizes and other prey items may be too small to be profitable (Zwarts and Blomert 1992; Piersma et al. 1993; Zwarts and Wanink 1993).

Many long-lived shorebird species demonstrate high site-fidelity (Marks and Redmond, 1996; Milsom et al., 2000; Finn et al., 2001). Individuals may not respond immediately to declines in feeding conditions, remaining in unprotected areas, or “ecological traps”, even when adjacent protected areas support higher prey densities where survival rates and individual body condition may be higher (Verhulst et al., 2004). A single winter after a change in shellfishery management is unlikely to provide strong signals of impacts to bird survival or fitness, for which temporal trends across years are much more representative (Cook et al., 2013). However this work gives a clear demonstration of the potential for these methods to be applied to these systems in the future, and to help inform adaptive management and ecosystem-based management of inshore fisheries with regards to management of protected sites and shorebird interests.

The current application of these methods as a means of quantifying fishing pressure in intertidal, and indeed subtidal habitats, is currently limited. Such methods may also be applied successfully in subtidal environments to characterise data obtained through Light Detection and Ranging (LiDAR) or side-scan sonar methods. Routinely collected aerial imagery can complement fisheries patrols, strongly increasing confidence in mapping fishing effort in inshore and intertidal fisheries and providing valuable information for management. This study was carried out in a remote intertidal channel in Poole Harbour surrounded by privately owned land where access is prohibited, hence the use of the UAS to obtain imagery from this site demonstrates their potential in obtaining valuable information from areas where access is difficult; the UAS used in this study was deployed from a publicly accessible nature reserve separated from the study site by large extents of intertidal mudflats. Where resources are limited and regular patrols to monitor fishing distribution are unfeasible or impractical, the methods investigated in this study may offer a low-cost solution for monitoring the extent and intensity of bottom-fishing in intertidal areas and subsequent impacts on biodiversity.

5. References

Atkinson, P.W., Clark, N.A., Bell, M.C., Dare, P.J., Clark, J.A., Ireland, P.L., 2003. Changes in commercially fished shellfish stocks and shorebird populations in the Wash, England. Biological Conservation 114, 127–141. https://doi.org/10.1016/S0006-3207(03)00017-X

Blaschke, T., Hay, G.J., Kelly, M., Lang, S., Hofmann, P., Addink, E., Feitosa, R.Q., Van der Meer, F., Van der Werff, H., Van Coillie, F., 2014. Geographic object-based image analysis–towards a new paradigm. ISPRS journal of photogrammetry and remote sensing 87, 180–191.

Bowgen, K.M., Stillman, R.A., Herbert, R.J.H., 2015. Predicting the effect of invertebrate regime shifts on wading birds: Insights from Poole Harbour, UK. Biological Conservation 186, 60–68. https://doi.org/10.1016/j.biocon.2015.02.032

Clarke, L.J., Esteves, L.S., Stillman, R.A., Herbert, R.J.H., 2018. Impacts of a novel shellfishing gear on macrobenthos in a marine protected area: pump-scoop dredging in Poole Harbour, UK. Aquat. Living Resour. 31, 5. https://doi.org/10.1051/alr/2017044

Clarke, L.J., Hughes, K.M., Esteves, L.S., Herbert, R.J.H., Stillman, R.A., 2017. Intertidal invertebrate harvesting: a meta-analysis of impacts and recovery in an important waterbird prey resource. Mar. Ecol.-Prog. Ser. 584, 229–244. https://doi.org/10.3354/meps12349

Collie, J.S., Hall, S.J., Kaiser, M.J., Poiner, I.R., 2000. Journal of Animal A quantitative analysis of fishing impacts on shelf-sea. Journal of Animal Ecology 69, 785–798.

Connor, D.W., Allen, J.H., Golding, N., Howell, K.L., Lieberknecht, L.M., Northen, K.O., Reker, J.B., 2004. The Marine Habitat Classification for Britain and Ireland Version 04.05-Sublittoral Sediment Section. Peterborough: Joint Nature Conservation Committee (JNCC).

dit Durell, S.E.L.V., Stillman, R.A., Caldow, R.W., McGrorty, S., West, A.D., Humphreys, J., 2006. Modelling the effect of environmental change on shorebirds: a case study on Poole Harbour, UK. Biological Conservation 131, 459–473.

Drone Deploy, 2018. https://www.dronedeploy.com/ Last Accessed: 24th October 2018.

Dunton, K.H., Schonberg, S.V., 2002. Assessment of propeller scarring in seagrass beds of the south Texas coast. Journal of Coastal Research 100–110.

Ens, B.J., 2006. The conflict between shellfisheries and migratory waterbirds in the Dutch Wadden Sea. GC Boere, CA Galbraith, and DA Stroud (red.), Waterbirds around the world 806–811.

Ens, B.J., Goss-Custard, J.D., 1986. Piping as a display of dominance by wintering Oystercatchers Haematopus ostralegus. Ibis 128, 382–391.

ESRI, 2018. ArcGIS Desktop Help. IsoCluster. http://webhelp.esri.com/arcgisdesktop/9.3/index.cfm?id=6273&pid=6263&topicname=Iso_Cluster Last Accessed: 24th October 2018.

Finn, P.G., Catterall, C.P., Driscoll, P.V., 2001. The low tide distribution of Eastern Curlew on feeding grounds in Moreton Bay, Queensland. Stilt 38, 9–17.

Foody, G.M., 2002. Status of land cover classification accuracy assessment. Remote sensing of environment 80, 185–201.

Goss-Custard, J.D., Stillman, R.A., West, A.D., Caldow, R.W.G., Triplet, P., Dit Durell, S.L.V., McGrorty, S., 2004. When enough is not enough: shorebirds and shellfishing. Proceedings of the Royal Society of London B: Biological Sciences 271, 233–237.

Goss-Custard, J.D., West, A.D., Yates, M.G., Caldow, R.W.G., Stillman, R.A., Bardsley, L., Castilla, J., Castro, M., Dierschke, V., Durell, S.E.A., Eichhorn, G., Ens, B.J., Exo, K.-M., Udayangani-Fernando, P.U., Ferns, P.N., Hockey, P.A.R., Gill, J.A., Johnstone, I., Kalejta-Summers, B., Masero, J.A., Moreira, F., Nagarajan, R.V., Owens, I.P.F., Pacheco, C., Perez-Hurtado, A., Rogers, D., Scheiffarth, G., Sitters, H., Sutherland, W.J., Triplet, P., Worrall, D.H., Zharikov, Y., Zwarts, L., Pettifor, R.A., 2006. Intake rates and the functional response in shorebirds (Charadriiformes) eating macro-invertebrates. Biological Reviews 81, 501–529. https://doi.org/10.1111/j.1469-185X.2006.tb00216.x

Hall, F.G., Botkin, D.B., Strebel, D.E., Woods, K.D., Goetz, S.J., 1991. Large-scale patterns of forest succession as determined by remote sensing. Ecology 72, 628–640.

Herbert, R.J., Ross, K., Huebner, R., Stillman, R.A., 2010. Intertidal invertebrates and biotopes of Poole Harbour SSSI and survey of Brownsea Island Lagoon.

Jensen, A.C., Humphreys, J., Caldow, R.W.G., Grisley, C., Dyrynda, P.E.J., 2004. Naturalization of the Manila clam (Tapes philippinarum), an alien species, and establishment of a clam fishery within Poole Harbour, Dorset. Journal of the Marine Biological Association of the UK 84, 1069–1073. https://doi.org/10.1017/S0025315404010446h

Kaiser, M., Clarke, K., Hinz, H., Austen, M., Somerfield, P., Karakassis, I., 2006. Global analysis of response and recovery of benthic biota to fishing. Marine Ecology Progress Series 311, 1–14. https://doi.org/10.3354/meps311001

Kenny, A.J., Cato, I., Desprez, M., Fader, G., Schüttenhelm, R.T.E., Side, J., 2003. An overview of seabed-mapping technologies in the context of marine habitat classification. ICES Journal of Marine Science 60, 411–418.

Marks, J.S., Redmond, R.L., 1996. Demography of bristle-thighed curlews Numenius tahitiensis wintering on Laysan Island. Ibis 138, 438–447.

Martín, J., Puig, P., Palanques, A., Ribó, M., 2014. Trawling-induced daily sediment resuspension in the flank of a Mediterranean submarine canyon. Deep Sea Research Part II: Topical Studies in Oceanography 104, 174–183.

Mason, D.C., Scott, T.R., Dance, S.L., 2010. Remote sensing of intertidal morphological change in Morecambe Bay, UK, between 1991 and 2007. Estuarine, Coastal and Shelf Science 87, 487–496.

McCluskey, S.M., Lewison, R.L., 2008. Quantifying fishing effort: a synthesis of current methods and their applications: Quantifying fishing effort: methods review. Fish and Fisheries 9, 188–200. https://doi.org/10.1111/j.1467-2979.2008.00283.x

Milsom, T.P., Langton, S.D., Parkin, W.K., Peel, S., Bishop, J.D., Hart, J.D., Moore, N.P., 2000. Habitat models of bird species' distribution: an aid to the management of coastal grazing marshes. Journal of Applied Ecology 37, 706–727.

Nagendra, H., Lucas, R., Honrado, J.P., Jongman, R.H., Tarantino, C., Adamo, M., Mairota, P., 2013. Remote sensing for conservation monitoring: Assessing protected areas, habitat extent, habitat condition, species diversity, and threats. Ecological Indicators 33, 45–59.

Phinn, S., Roelfsema, C., Dekker, A., Brando, V., Anstee, J., 2008. Mapping seagrass species, cover and biomass in shallow waters: An assessment of satellite multi-spectral and airborne hyper-spectral imaging systems in Moreton Bay (Australia). Remote sensing of Environment 112, 3413–3425.

Piersma, T., Koolhaas, A., Dekinga, A., 1993. Interactions between stomach structure and diet choice in shorebirds. The Auk 552–564.

Quattrochi, D.A., Goodchild, M.F., 1997. Scale in remote sensing and GIS. CRC press.

Robbins, B.D., 1997. Quantifying temporal change in seagrass areal coverage: the use of GIS and low resolution aerial photography. Aquatic Botany 58, 259–267.

Stillman, R.A., Goss-Custard, J.D., West, A.D., Durell, S.L.V.D., McGrorty, S., Caldow, R.W.G., Norris, K.J., Johnstone, I.G., Ens, B.J., Van der Meer, J., 2001. Predicting shorebird mortality and population size under different regimes of shellfishery management. Journal of Applied Ecology 38, 857–868.

Stillman, R.A., Wood, K.A., 2013. Towards a simplified approach for assessing bird food requirements on shellfisheries. A report to the Welsh Government.

Thomson, A.G., Fuller, R.M., Yates, M.G., Brown, S.L., Cox, R., Wadsworth, R.A., 2003. The use of airborne remote sensing for extensive mapping of intertidal sediments and saltmarshes in eastern England. International Journal of Remote Sensing 24, 2717–2737.

Turner, W., Spector, S., Gardiner, N., Fladeland, M., Sterling, E., Steininger, M., 2003. Remote sensing for biodiversity science and conservation. Trends in Ecology and Evolution 18, 306–314.

Verhulst, S., Oosterbeek, K., Rutten, A.L., Ens, B.J., 2004. Shellfish Fishery Severely Reduces Condition and Survival of Oystercatchers Despite Creation of Large Marine Protected Areas. Ecology and Society 9. https://doi.org/10.5751/ES-00636-090117

Wood, E.M., Pidgeon, A.M., Radeloff, V.C., Keuler, N.S., 2012. Image texture as a remotely sensed measure of vegetation structure. Remote Sensing of Environment 121, 516–526.

Wood, E.M., Pidgeon, A.M., Radeloff, V.C., Keuler, N.S., 2013. Image texture predicts avian density and species richness. PloS one 8, e63211.

Woodcock, C.E., Strahler, A.H., 1987. The factor of scale in remote sensing. Remote sensing of Environment 21, 311–332.

Zharikov, Y., Skilleter, G.A., 2004. Potential interactions between humans and non-breeding shorebirds on a subtropical intertidal flat. Austral Ecology 29, 647–660.

Zwarts, L., Blomert, A.-M., 1992. Why knot Calidris canutus take medium-sized Macoma balthica when six prey species are available. Marine Ecology Progress Series 113–128.

Zwarts, L., Wanink, J.H., 1993. How the food supply harvestable by waders in the Wadden Sea depends on the variation in energy density, body weight, biomass, burying depth and behaviour of tidal-flat invertebrates. Netherlands Journal of Sea Research 31, 441–476.

6. Figures

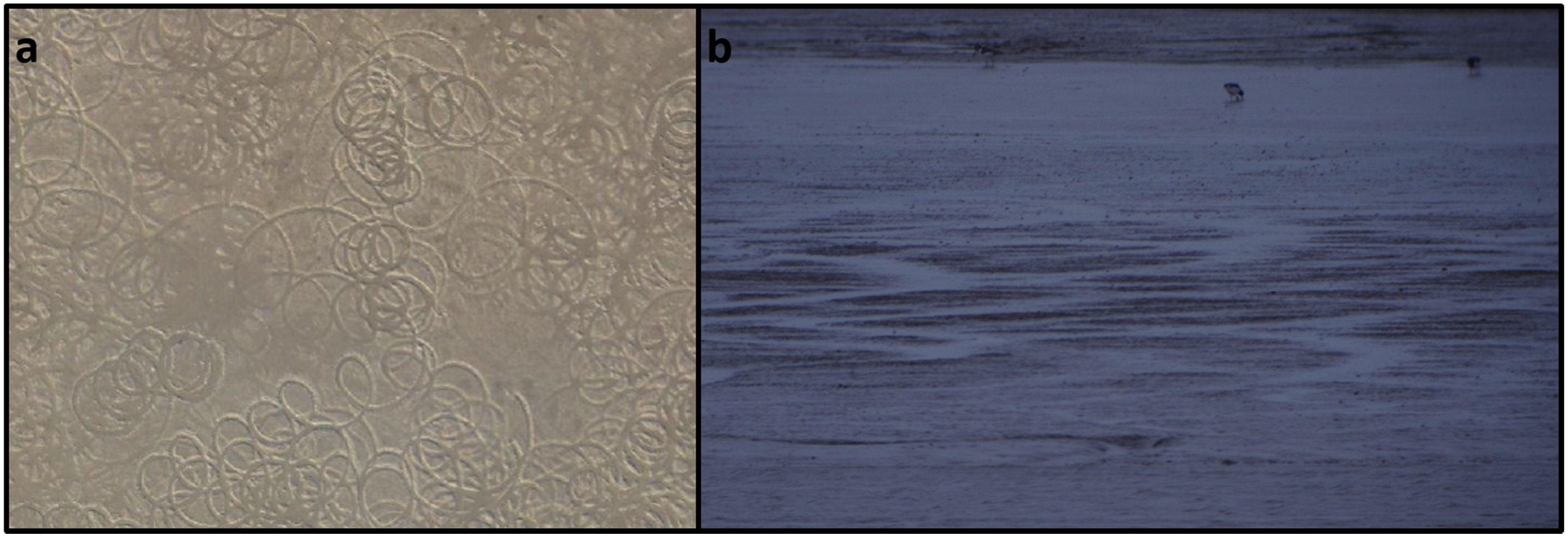

Figure 1 Scarring of intertidal sediments in Wytch Lake, Poole Harbour resulting from pump-scoop dredging observed from (a) aerial imagery and (b) imagery taken from the shoreline. Feeding oystercatcher *Haematopus ostralegus* can be seen feeding in the background in (b).

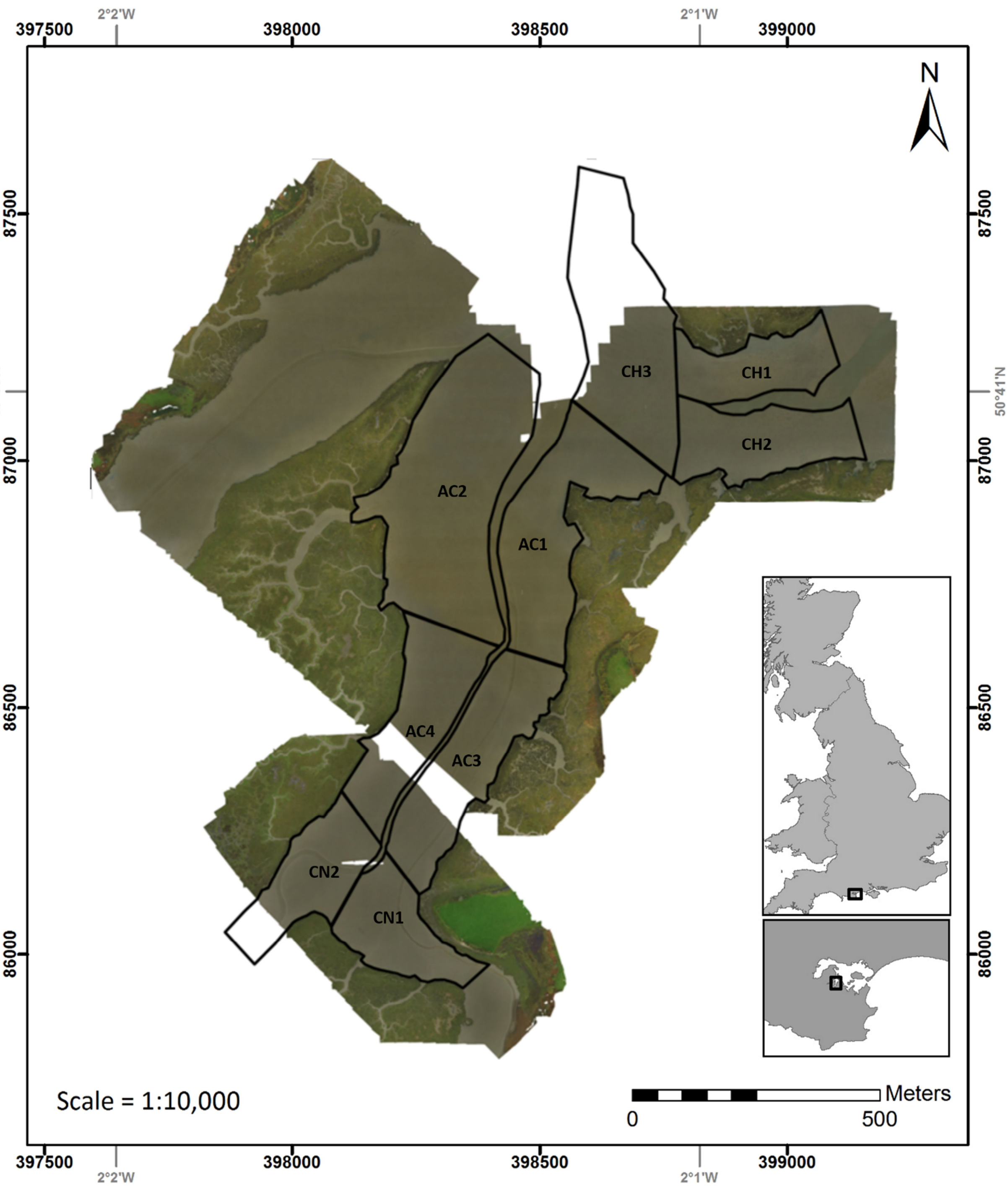

Figure 2. Aerial imagery of Wytch Lake obtained at low tide on November 23rd 2015 with the nine survey sectors outlined. CH = chronic dredging pressure; AC = acute, short-term dredging pressure, CN = control. White areas indicate no data, which were cut from the image before analyses were undertaken. Biotopes across the study site classified according to Connor et al. (2004) include polychaete and bivalve dominated

mid estuarine muds (LS.LMu.MEst) and *Hediste diversicolor* and *Macoma balthica* in littoral sandy mud (LS.LMu.MEst.HedMac).

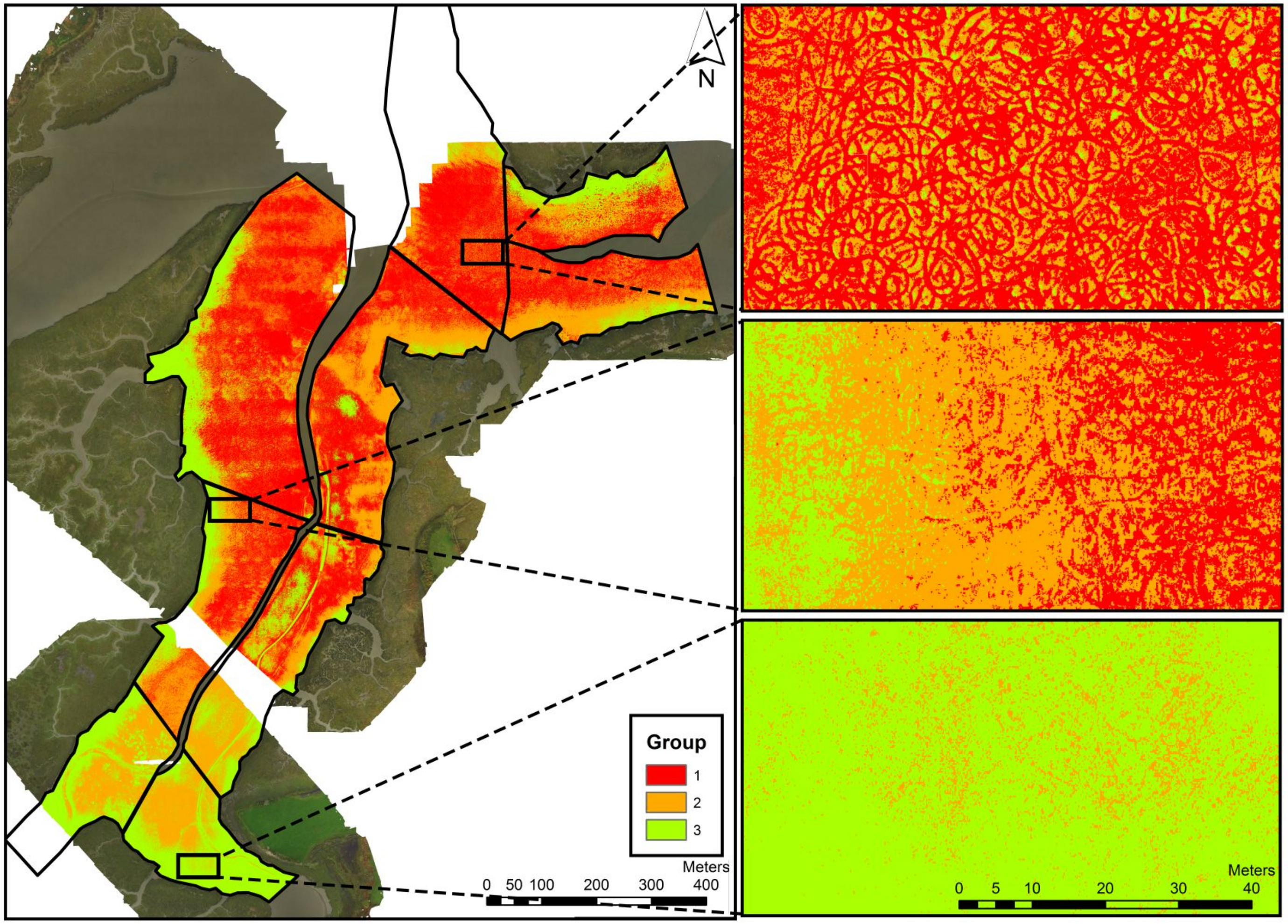

Figure 3. Results of the unsupervised image classification process. The extent of each raster band in each of the survey sectors is evident. The magnified images on the right correspond to the extent indicators on the main map of the survey site. Round Island is the area immediately to the north of survey sector CH1. Group 1:

Estimated > 90% pixels correctly classified as disturbed or scarred sediment. High confidence in classification; Group 2: Estimated 50% pixels correctly classified. Intermediate confidence in classification; Group 3: Estimated > 90% pixels correctly classified as undisturbed sediment. High confidence in classification.

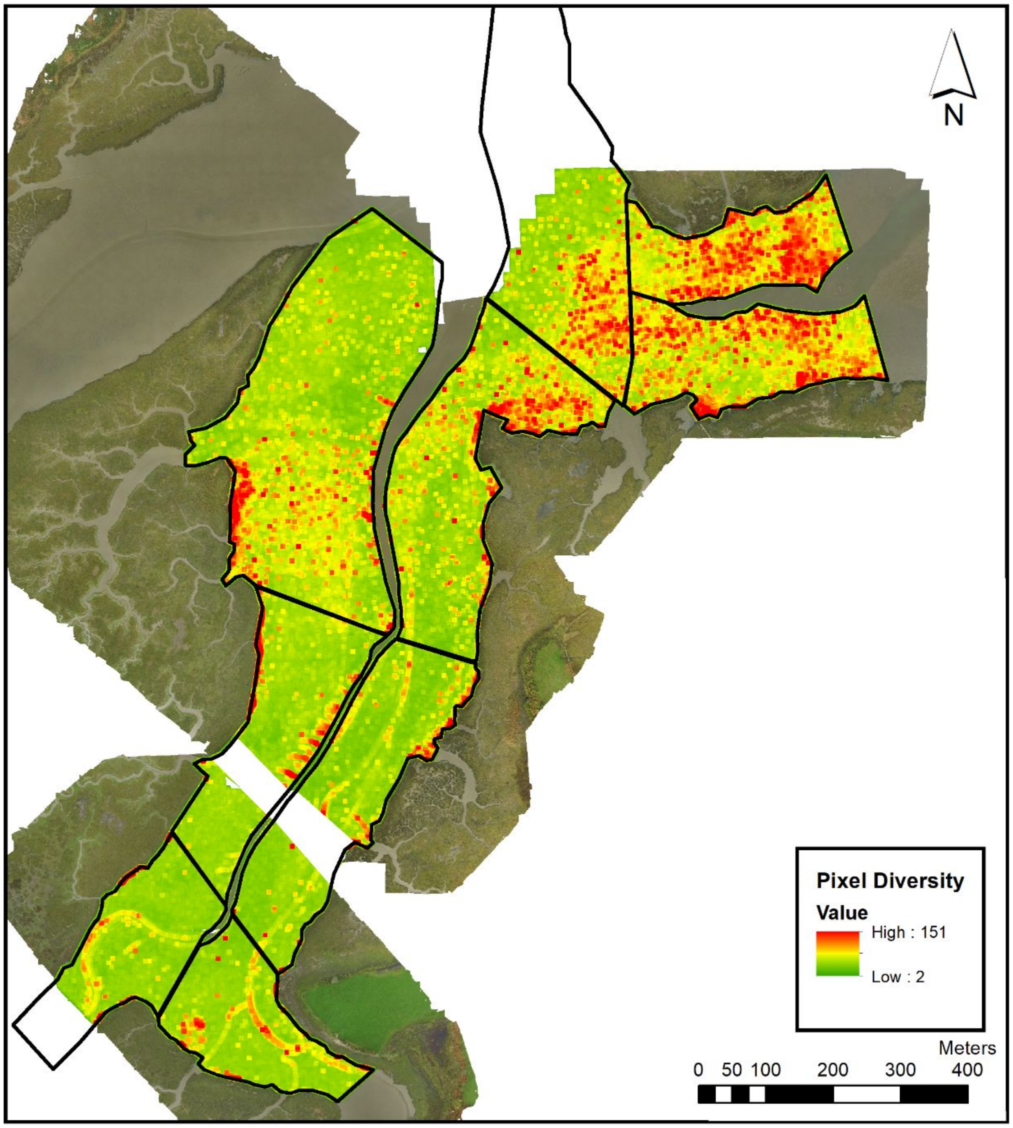

704

705 **Figure 4. Results of the image texture analysis, displayed as pixel diversity values ranging from high (red) to**

706 **low diversity values (green) across a 200 x 200 pixel (7m x 7m) grid.**

707

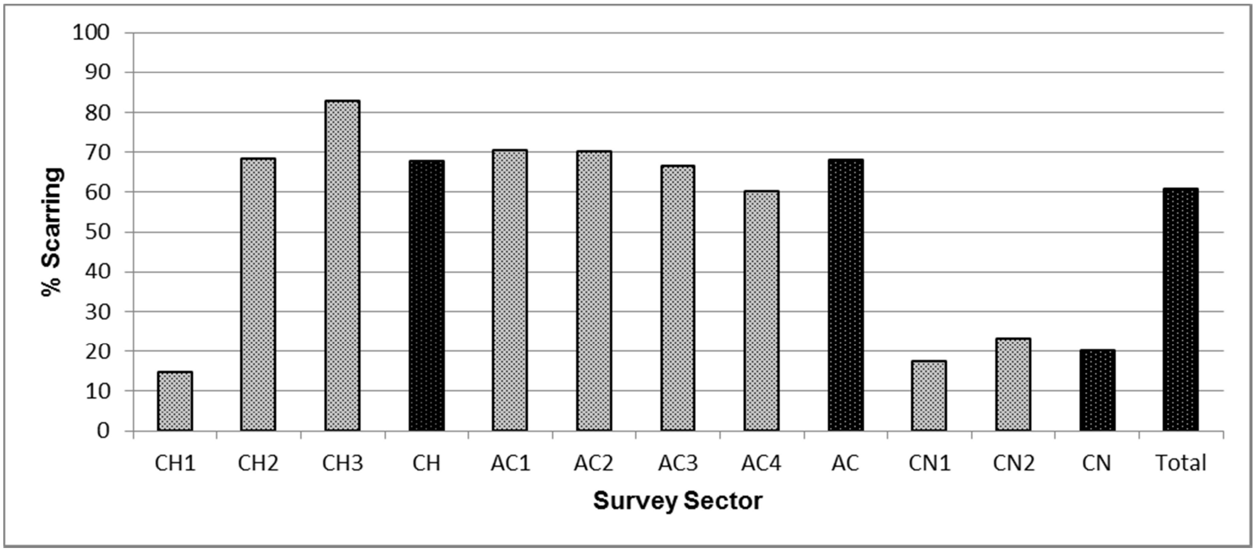

Figure 5. Percentage of each survey sector scarred by pump-scoop dredging derived from the unsupervised image classification. Dark grey bars indicate values for whole sites. CH = chronic dredging pressure; AC = acute, short-term dredging pressure, CN = control.

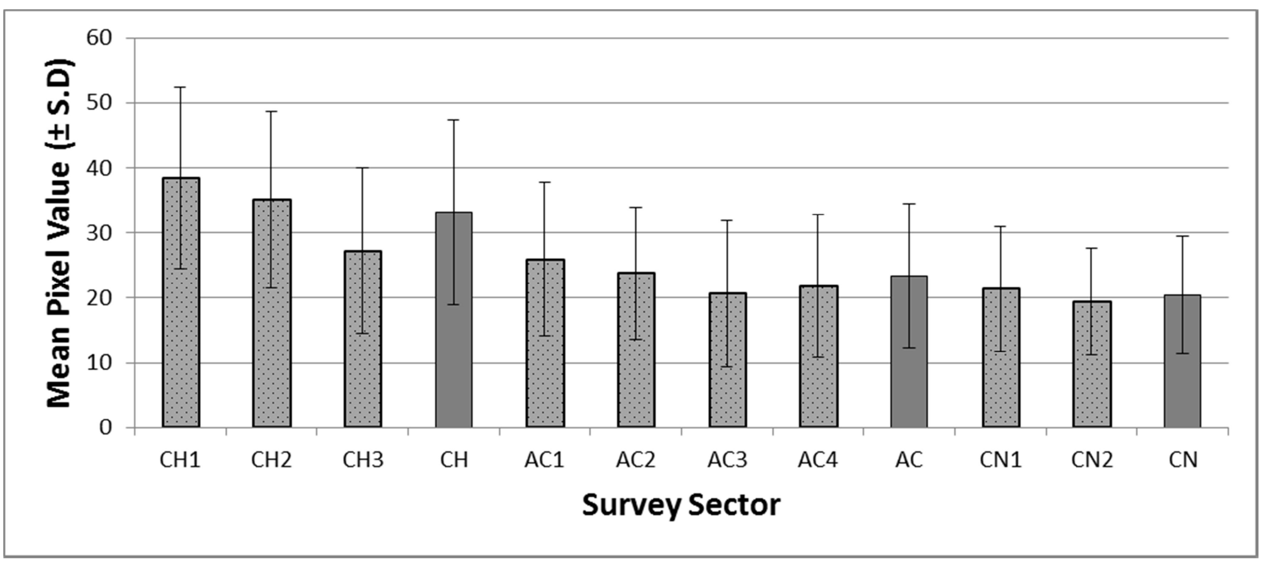

Figure 6. Mean (± S.D.) diversity value of pixels in each survey sector derived from the image texture analysis method. Dark grey bars indicate values for whole sites. CH = chronic dredging pressure; AC = acute, short-term dredging pressure, CN = control.

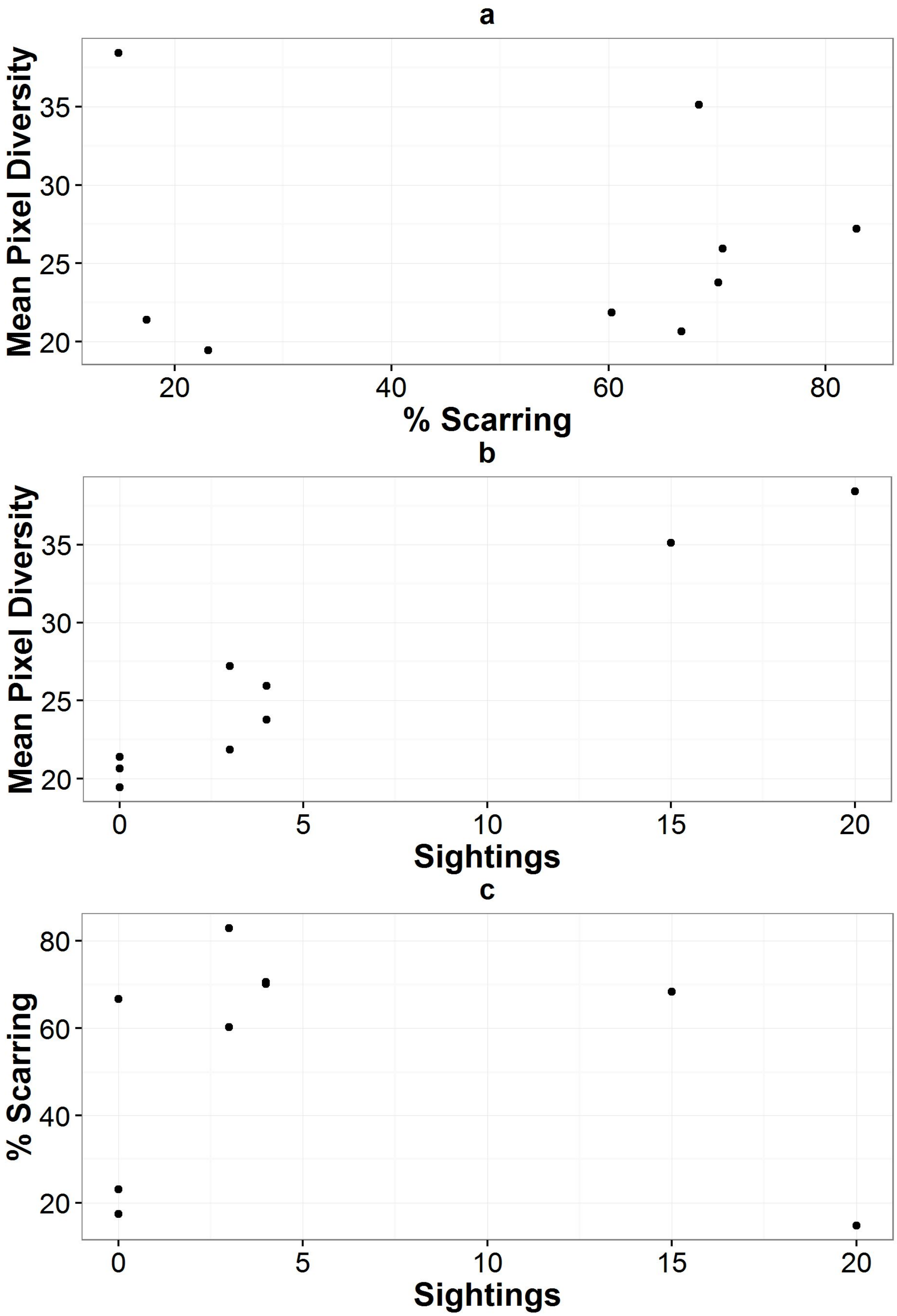

Figure 7. a) Mean pixel diversity plotted against % scarred sediment; b) no. fishing sightings vs. mean pixel diversity; and c) no. fishing sightings vs. % scarred sediment for each survey sector.

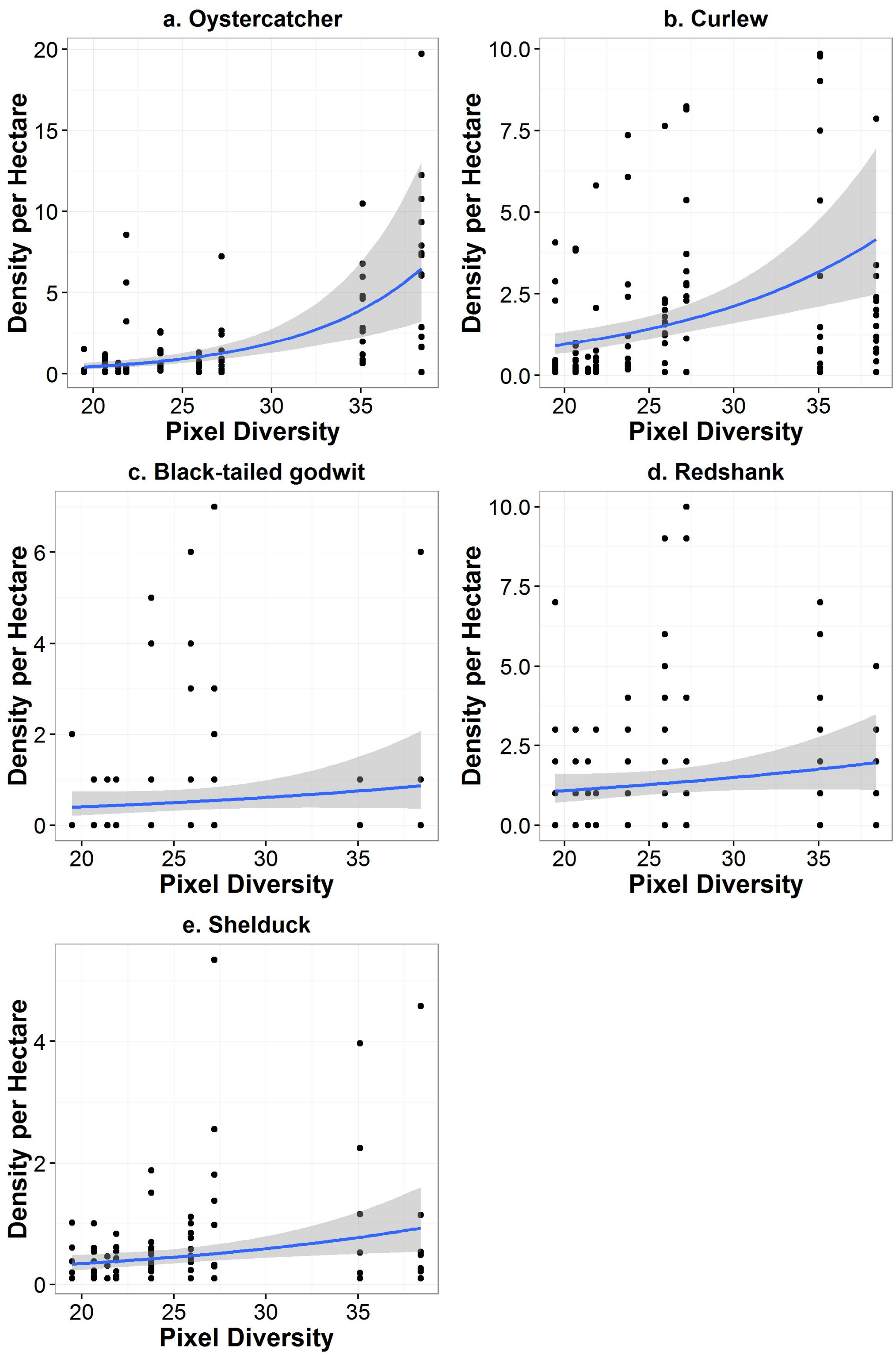

Figure 8. Generalised linear models of species densities against pixel diversities as a proxy for sediment disturbance.

7. Tables

Table 1. Fishing intensity and seasonal openings of each site sampled under the dredge permit byelaw, which came in to force on 1st July 2015

Site	Fishing Intensity	Pre-byelaw	Post-byelaw
Control (CN)	Low (none)	Closed	Closed
Acute Dredging (AC)	Acute/Medium	Closed	Open (1st July - 31st October)
Chronic Dredging (CH)	Chronic/Heavy	Open	Open (25th May - 24th December)

Table 2. Inclusion criteria for each of the three groups into which output classes from the unsupervised classification were included. The scale factor applied to each group to calculate an estimate of spatial extent of scarring is indicated.

Group	Class Selection Criteria	Scale Factor
1	Estimated > 90% pixels correctly classified as disturbed or scarred sediment. High confidence in classification.	1
2	Estimated 50% pixels correctly classified. Intermediate confidence in classification.	0.5
3	Estimated > 90% pixels correctly classified as undisturbed sediment. High confidence in classification.	0

Table 3. Measures of dredging extent derived from the image classification process described above, including the estimate for each class using the scale factors from Table 2. Sector labels denoted with * indicate areas where data is missing and values are calculated using available data only.

Management Area (fishing pressure)	Sector Label	Recoded Image Class	Area (hectares)	Percentage Cover (%)	Scarring Estimate (hectares)	Scarring Estimate (%)	Estimated Total % Scarred
		1	1.33	10.03	1.33	10.03	
	CH1	2	1.27	9.59	0.63	4.79	**14.82**
		3	10.63	80.38	0.00	0.00	
		1	20.83	43.84	20.83	43.84	
Chronic	CH2	2	23.26	48.97	11.63	24.49	**68.33**
		3	3.42	7.19	0.00	0.00	
		1	31.79	69.15	31.79	69.15	
	CH3*	2	12.57	27.33	6.28	13.67	**82.82**
		3	1.62	3.51	0.00	0.00	
		1	**53.94**	**50.55**	**53.94**	**50.55**	
Area Total	**CH**	**2**	**37.10**	**34.77**	**18.55**	**17.38**	**67.94**
		3	**15.66**	**14.68**	**0.00**	**0.00**	
		1	35.64	47.33	35.64	47.33	
	AC1	2	34.91	46.36	17.46	23.18	**70.52**
		3	4.75	6.30	0.00	0.00	
		1	72.64	57.27	72.64	57.27	
	AC2*	2	32.61	25.71	16.31	12.85	**70.12**
		3	21.60	17.03	0.00	0.00	
Acute		1	27.79	48.63	27.79	48.63	
	AC3*	2	20.67	36.16	10.33	18.08	**66.71**
		3	8.70	15.22	0.00	0.00	
		1	17.72	36.40	17.72	36.40	
	AC4*	2	23.25	47.75	11.62	23.87	**60.27**
		3	7.72	15.86	0.00	0.00	

Area Total	**AC**	**1**	**153.80**	**49.94**	**153.80**	**49.94**	**68.03**
		2	**111.43**	**36.18**	**55.72**	**18.09**	
		3	**42.76**	**13.88**	**0.00**	**0.00**	
Control	CN1	1	0.00	0.00	0.00	0.00	**17.42**
		2	13.54	34.83	6.77	17.42	
		3	25.34	65.17	0.00	0.00	
	CN2*	1	0.00	0.00	0.00	0.00	**23.08**
		2	16.27	46.16	8.14	23.08	
		3	18.98	53.84	0.00	0.00	
Area Total	**CN**	**1**	**0.00**	**0.00**	**0.00**	**0.00**	**20.11**
		2	**29.81**	**40.22**	**14.91**	**20.11**	
		3	**44.32**	**59.78**	**0.00**	**0.00**	
Study Site Total	**All**	**1**	**207.74**	**42.50**	**207.74**	**42.50**	**60.74**
		2	**178.35**	**36.48**	**89.17**	**18.24**	
		3	**102.74**	**21.02**	**0.00**	**0.00**	

Table 4. Zonal statistics for each individual survey sector. Each statistic is derived from the pixel diversity values of the output raster from the moving window neighbourhood analysis described in the methods.

Site	Survey Sector	Min	Max	Range	Mean (± S.D.)	S.E.	Variety	Majority	Minority	Median
CH	CH1	13	140	127	38.41 ± 14.00	0.0026	128	25	13	36
	CH2	14	134	120	35.11 ± 13.52	0.0022	121	28	116	32
	CH3	2	151	149	27.20 ± 12.73	0.0020	150	17	99	23
	Area Total	**2**	**151**	**149**	**33.18 ± 14.17**	**0.0014**	**150**	**26**	**135**	**30**
AC	AC1	10	127	117	25.93 ± 11.81	0.0015	118	17	124	22
	AC2	2	113	111	23.76 ± 10.17	0.0001	112	18	101	21
	AC3	2	120	118	20.66 ± 11.23	0.0016	119	15	117	17
	AC4	2	109	107	21.86 ± 10.99	0.0016	108	18	108	19
	Area Total	**2**	**127**	**125**	**23.33 ± 11.09**	**0.0001**	**126**	**17**	**124**	**20**
CN	CN1	12	82	70	21.39 ± 9.65	0.0017	71	17	79	18
	CN2	2	88	86	19.47 ± 8.24	0.0015	87	16	87	17
	Area Total	**2**	**88**	**86**	**20.46 ± 9.04**	**0.0012**	**87**	**16**	**87**	**17**

Table 5. Outputs from best-fit generalised linear models to assess the effect of predictor variables on species distributions throughout the study site in winter 2015/16.

Oystercatcher						
Model	**Parameter**	**Estimate**	**S.E.**	**Test Statistic**	**Probability**	**Theta**
Density ~ Pixel Diversity + Days Through Winter + LW Height	Pixel Diversity	0.182	0.216	8.436	**< 0.001**	1.16
	Days Through Winter	-0.004	0.002	-2.007	**< 0.05**	
	LW Height	1.718	0.516	3.328	**< 0.01**	
Curlew						
Model	**Parameter**	**Estimate**	**S.E.**	**Test Statistic**	**Probability**	**Theta**
Density ~ Pixel Diversity + LW Height	Pixel Diversity	0.118	0.019	6.262	**< 0.001**	1.48
	LW Height	0.624	0.453	3.585	**< 0.001**	
Black-tailed godwit						
Model	**Parameter**	**Estimate**	**S.E.**	**Test Statistic**	**Probability**	**Theta**
Density ~ Pixel Diversity + Days Through Winter + LW Height	Pixel Diversity	0.007	0.031	0.219	0.826	0.48
	Days Through Winter	-0.005	0.003	-1.814	0.070	
	LW Height	-3.276	0.818	-4.006	**< 0.001**	
Redshank						
Model	**Parameter**	**Estimate**	**S.E.**	**Test Statistic**	**Probability**	**Theta**

Density ~ Pixel Diversity + Days Through Winter	Pixel Diversity	0.033	0.020	1.683	0.092	0.92
	Days Through Winter	0.011	0.002	4.728	**< 0.001**	
Shelduck						
Model	**Parameter**	**Estimate**	**S.E.**	**Test Statistic**	**Probability**	**Theta**
Density ~ Pixel Diversity	Pixel Diversity	0.054	0.020	2.681	**< 0.01**	1.29

Table 6. Effect of image pixel diversity (as a proxy for fishing intensity) on feeding rate and intake rates in each species. Results represent outputs of best-fit GLMs.

Species	Response	Estimate	S.E.	Test Statistic	Probability
Oystercatcher	**Feeding Rate**	0.010	0.013	0.800	0.425
	Intake Rate	0.021	0.007	3.249	**< 0.01**
Black-tailed godwit	**Feeding Rate**	-0.032	0.014	-2.242	**< 0.05**
	Intake Rate	-0.003	0.002	-1.454	0.150
Curlew	**Feeding Rate**	-0.033	0.012	-2.962	**< 0.01**
	Intake Rate	0.001	0.004	0.179	0.858